Scanning Tunneling Microscopy Study of the Thick Film Limit of Kinetic Roughening

Palasantzas, G.; Krim, J.

Published in:
Physical Review Letters

DOI:
10.1103/PhysRevLett.73.3564

Publication date:
1994

Scanning Tunneling Microscopy Study of the Thick Film Limit of Kinetic Roughening

G. Palasantzas and J. Krim
Physics Department, Northeastern University, Boston, Massachusetts 02115
(Received 16 December 1993)

The spatial and temporal scaling behaviors of vapor-deposited silver films have been investigated by means of scanning tunneling microscopy for the film thickness range $\approx$10–1000 nm. The roughness, growth, and dynamic scaling exponents have been independently measured ($\alpha = 0.82 \pm 0.05, \beta = 0.29 \pm 0.06$, and $z = 2.5 \pm 0.5$), and they exhibit no evolution with film thickness.

PACS numbers: 68.55.Jk, 64.60.–i, 68.90.+g

A wide variety of surfaces and interfaces occurring in nature are well represented by a kind of roughness associated with self-affine fractal scaling, defined by Mandelbrot in terms of fractional Brownian motion [1]. Whether similar surface morphologies formed by distinctly different physical processes have in fact common basis is a question which remains unanswered. The area of nonequilibrium film growth, and the surface roughness associated with it, shows great promise for illuminating this issue.

All rough surfaces exhibit perpendicular fluctuations which are characterized by an rms width $\sigma = \langle z(x,y)^2\rangle^{1/2}; z(x,y) = h(x,y) - \langle h(x,y)\rangle$, where $h(x,y)$ is the height function and $\langle\cdots\rangle$ is the spatial average over a planar reference surface. Films grown under nonequilibrium conditions are expected to develop self-affine surfaces [2], whose rms widths scale with time t and the length L sampled as [3]

$$\sigma(L,t) = L^{\alpha} F(t/L^{\alpha/\beta}), \tag{1}$$

where $\sigma(L) \propto L^{\alpha}$ for $t/L^{\alpha/\beta} \to \infty$ and $\sigma(t) \propto t^{\beta}$ for $t/L^{\alpha/\beta} \to 0$. The parameter $0 < \alpha < 1$ is the "static scaling," or "roughness" exponent [4], and the parameter β is the "growth" exponent. Actual self-affine surfaces are characterized by an upper horizontal cutoff to scaling, or correlation length ξ, beyond which the surface width no longer scales as L^{α}, and eventually reaches a saturation value σ. Implicit in Eq. (1) is a correlation length which increases with time as $\xi \propto t^{1/z}$, where $z = \alpha/\beta$ is the "dynamic" scaling exponent.

Theoretical treatments of nonequilibrium film growth typically employ partial differential equations involving phenomenological expansions in the derivatives of a time dependent height function $h(x,y,t)$. The Kardar-Parisi-Zhang (KPZ) equation [5] is one well-known example of this approach where there is a consensus between continuum theory and numerical simulation, yielding $\alpha = 0.3$–0.4, $\beta = 0.24$–0.25 for growth on a two-dimensional surface [6]. The KPZ equation does not conserve particle number, and so it applies to cases where desorption and/or vacancy formation, but not surface diffusion, are the dominant surface relaxation mechanisms. In efforts to realistically treat surface diffusion, a number of conservative continuum equations have been proposed [7]. The various models predict distinctly different values for the scaling exponents and frequently predict "crossover behavior" for the exponents, i.e., an evolution in their values with film thickness [8–10]. Investigating whether the exponents evolve with film thickness is clearly in order, since firm evidence for their evolution would imply reevaluation of most, if not all, prior experimental work in this area.

Previous experimental investigations which have reported values for both α and β [11–15] have generally not reported their thickness dependence or their asymptotic values. You *et al.* [11] measured α for one film thickness and one deposition condition, while Thompson *et al.* [12] measured α with precision too low to establish a thickness dependency. He *et al.* [13] and Ernst *et al.* [14] studied films too thin to establish asymptotic values. We report here a scanning tunneling microscopy (STM) study of the thickness dependence of all three of the scaling exponents, for vapor-deposited Ag/quartz. By independently measuring α and σ for *each* thickness studied in the range $\approx$10–1000 nm, we have established asymptotic values and ruled out any thickness dependencies of the scaling exponents. By measuring ξ for each film thickness studied, we have obtained an independent measure of the dynamic exponent z and confirmed the relation $z = \alpha/\beta$. Finally, by measuring roughness amplitudes in addition to the scaling exponents, we have documented some basic consistencies of the experimental results with theories to which they are being compared.

The Ag films studied here were deposited onto quartz in a deposition system previously employed for x-ray reflectivity studies of Ag/Si [12]. These, along with previous adsorption studies of Ag film growth on quartz [16], rule out any significant discrepancies in the surface area detected by the various techniques, confirming that tip curvature effects can be neglected. For example, the rms width of a 73 nm thick silver film determined by x-ray reflectivity measurements (3.0 nm) is within experimental error of that determined by STM (3.2 nm) [12]. Typical slopes for the film surfaces obtained by

 0031-9007/94/73(26)/3564(4)$06.00

STM are on the order of 10 deg, or approximately a 1.5% increase in surface area of the film with respect to that of a planar surface. This agrees with adsorption measurements, which indicated planar surfaces within the resolution of the technique [16]. The x-ray and adsorption results establish that bulk vacancies and/or surface overhangs are negligible, so that surface diffusion of the incoming Ag atoms is the only viable relaxation mechanism. The deposition nonetheless occurs under nonequilibrium growth conditions, since surface diffusion of Ag is clearly limited at room temperature [17].

The films were produced by thermal evaporation of 99.999% pure Ag at normal incidence, 10^{-7}–10^{-8} Torr and 0.03 nm/s onto an optically polished quartz substrate, which was cleaned between depositions. The parameters α, ξ, and σ were obtained from STM images recorded in dry N_2 with a Digital Instruments Nanoscope II, at grid density 400×400 ($I \approx 0.75$ na, $V \approx 50$ mV). Typical images are displayed in Fig. 1.

Two analysis approaches are presented in Fig. 2, for a sample which is represented by circles at $h = 208$ nm in Fig. 3. The first approach involves the correlation functions $g(R) = \langle [z(x', y') - z(x, y)]^2 \rangle$ and $C(R) = \langle z(R)z(0) \rangle = \sigma^2 - g(R)/2; R = \sqrt{(x - x')^2 + (y - y')^2}$, where the average is taken over pairs of points which are separated horizontally by the length R. If the surface is self-affine with a finite correlation length, then $g(R) \propto R^{2\alpha}$ as $R \to 0$ and $g(R) = 2\sigma^2$ as $R \to \infty$. Correlation data were obtained from five 700×700 $(\text{nm})^2$ images recorded at random locations and then averaged. The value for ξ was obtained by assuming the analytic form for the height-height correlation function [18], $C(R) = \sigma^2 e^{-(R/\xi)^{2\alpha}}$, where $C(\xi) = C(0)/e$. The exponent α was obtained from the slope of a log-log plot of $g(R)$ vs R in the range $0 < R < 0.4\xi$. The value for σ was taken from scans where $L \geq 20\xi$. For the data presented in Fig. 2, this procedure yielded $\xi = 24$ nm, $\alpha = 0.84 \pm 0.06$, and $\sigma = 2.88$ nm.

The inset to Fig. 2 depicts a second analysis approach which involves direct measurement of the surface width as a function of scan size. The exponent α is obtained from the scaling behavior of $\sigma(L)$ for $L < \xi$, and σ is taken from scans where $L \geq 20\xi$. In order to assign a correlation length to the data, an analytic form for $\sigma(L)$ must be assumed. Taking the film thickness h to be directly proportional to the deposition time t, and defining $x = h/L^{\alpha/\beta}$, two forms for $\sigma(L, t)$ which satisfy the dynamic scaling conditions Eq. (1) are

$$\sigma_1(L, h) = L^{\alpha} A_1 (1 - e^{-A_2 x^{\beta}}); \quad \xi_1 = A_2^{1/\alpha} h^{\beta/\alpha}, \tag{2}$$

with $\sigma_1(L) = A_1 L^{\alpha}$ for $x \to \infty$ and $\sigma_1(h) = A_1 A_2 h^{\beta}$ for $x \to 0$, and

$$\sigma_2(L, h) = L^{\alpha} \frac{B_1 x^{\beta}}{(1 + B_2 x^{2\beta/\alpha})^{\alpha/2}}; \quad \xi_2 = \frac{\sqrt{B_2 \alpha/2}}{\pi} h^{\beta/\alpha}, \tag{3}$$

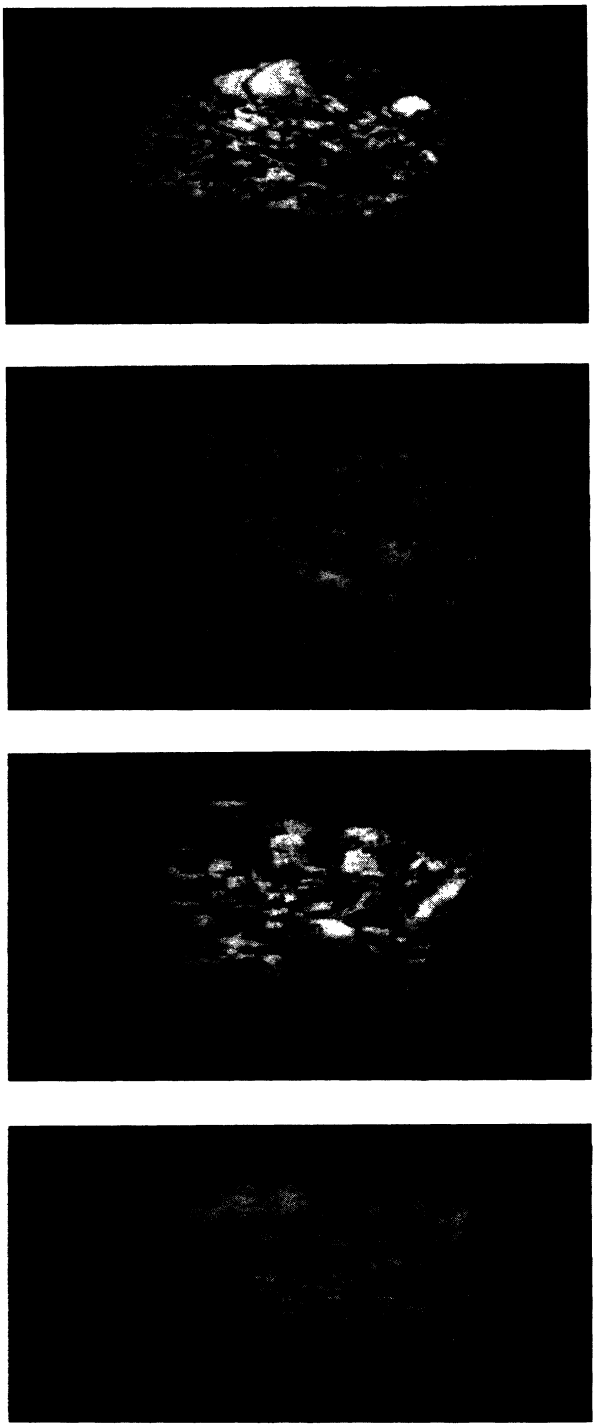

FIG. 1. Typical STM images for film thickness (top to bottom) $h = 50.2$, 147, 280, and 702 nm. The horizontal and vertical axes, respectively, range from 0 to 650 nm and 0 to 70 nm, so vertical fluctuations are magnified by approximately 3.

with $\sigma_2(L) = B_1 B_2^{-\alpha/2} L^{\alpha}$ for $x \to \infty$ and $\sigma_2(h) = B_1 h^{\beta}$ for $x \to 0$. These functions are represented by dashed (σ_1) and solid (σ_2) lines in the inset to Fig. 2, where the values for α and β are listed in Table I. The function $\sigma_2(L, h)$ provides the better description of the data and in

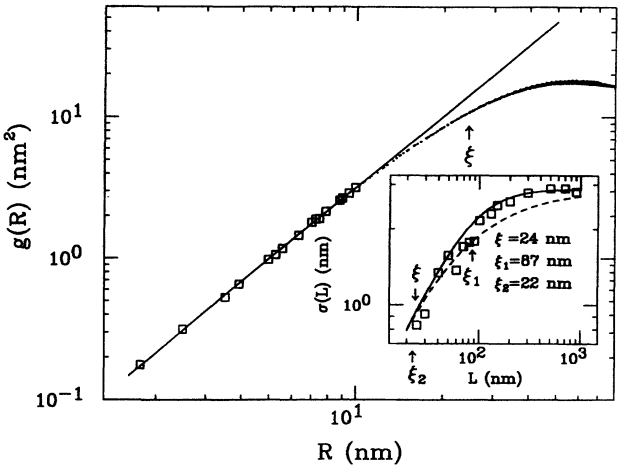

FIG. 2. Correlation $g(R)$ data for a 208 nm thick sample. The roughness exponent $\alpha = 0.84 \pm 0.06$ is obtained from a power law to fit to data in the regime $0 \leq R \leq 0.4\xi$, where R is the horizontal separation between pairs of points. The solid line has slope 2α. The inset presents rms width vs scan size $\sigma(L)$ data for the same film, fit to Eqs. (2) (dashes) and (3) (solid).

addition has an analytic form for $C(R)$ to which it can be mapped [19]. The correlation length $\xi_2 = 22$ nm obtained from $\sigma_2(L, h)$ is close to $\xi = 24$ nm. Both are on the order of the film's crystalline grain size, as determined from x-ray diffraction measurements [20].

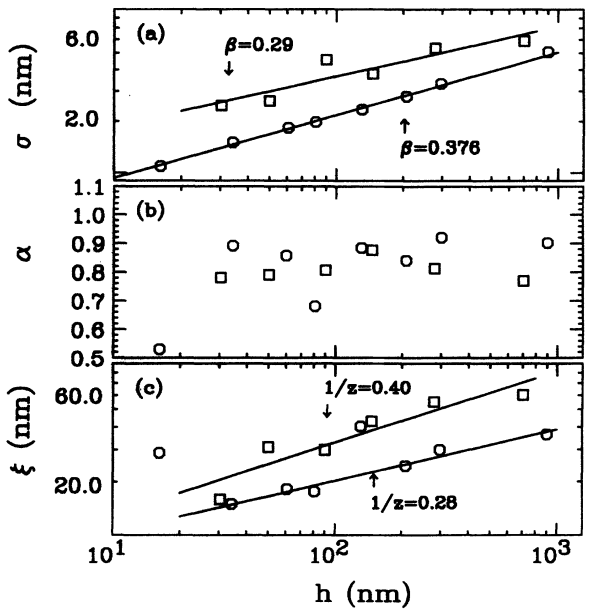

FIG. 3. Experimental results for two slightly different deposition conditions (see text) for the rms width σ, the roughness exponent α, and the correlation length ξ vs film thickness h. Data represented by squares are the primary results of this study. All solid lines represent least squares fits to the data, yielding the growth exponent β and the dynamic exponent z. (Values for ξ represented by circles at $h = 16$ and 131 nm were not included in the line fit.)

TABLE I. Summary of experimental results. All lengths are in nm (1 nm $\approx$ 4.3 layers). Data represented by squares are the primary results of this study.

	Fig. 3, squares	Fig. 3, circles
Range of h	30–700	16–900
α	0.82 ± 0.05	0.85 ± 0.09
β	0.29 ± 0.06	0.376 ± 0.007
z	2.5 ± 0.5	3.6 ± 0.3
α/β	2.8 ± 0.6	2.3 ± 0.25
$\xi(h)$	$\xi(h) = 5.31h^{0.40}$	$\xi(h) = 5.5h^{0.28}$
$h/L^{\alpha/\beta} \to \infty$	$\sigma(L) = 0.06L^{0.82}$	$\sigma(L) = 0.09L^{0.85}$
$h/L^{\alpha/\beta} \to 0$	$\sigma(h) = 0.956h^{0.29}$	$\sigma(h) = 0.385h^{0.376}$

The width vs scan size approach can easily be applied to samples which exhibit scaling over many orders of magnitude and is limited in precision only by the number of images which are averaged [21]. For the samples studied here, where ξ was limited *well* below that of the image size analyzed, the correlation analysis was quite suitable for determining all three parameters σ, α, and ξ. The values reported in Fig. 3 and Table I were obtained in this manner, since it involved fewer images. All points in Fig. 3(a) have been corrected for the rms width of the quartz substrate, $\sigma_{\text{quartz}} \approx 0.6$ nm, according to $\sigma_{\text{corrected}} = (\sigma^2 - \sigma^2_{\text{quartz}})^{1/2}$, affecting the reported values of β by less than 0.02. The squares in Fig. 3, and the second column of Table I are the primary results of this study.

We observe the exponents $\alpha = 0.82 \pm 0.05$, $\beta = 0.29 \pm 0.06$, and $z = 2.5 \pm 0.5$ to be constant to within experimental error, for all thicknesses studied. Since the error margins are narrow enough to rule out significant changes in their values before reaching macroscopic dimensions (if the data were extended further by two decades, the film thickness would be 0.1 mm), the exponents have arguably reached their asymptotic limits. Our values are close to those reported for Ag/Si at 300 K ($\beta = 0.26 \pm 0.05$; $\alpha = 0.70 \pm 0.10$) [12], Fe/Si(111) at 323 K ($\beta = 0.25 - 0.32$) [22], Fe/Fe(001) at 343 K ($\beta = 0.22 \pm 0.02$; $\alpha = 0.79 \pm 0.05$) [13], Cu/Cu(100) at 160 K ($\beta = 0.26$; $\alpha \approx 1$) [14] Au/glass at 300 K [23] ($\alpha = 0.89 \pm 0.05$ for $L < 38$ nm) and $CuCl/CaF_2(111)$ at 373 C [24] ($\alpha = 0.84 \pm 0.05$). Although none of these experiments tracked the evolution of the scaling exponents towards asymptotic limits, our results would indicate that the exponents may be taken as asymptotically limiting values.

While it is clear that a broad range of homoepitaxial and heteroepitaxial growth conditions (but certainly not all) yield scaling exponents in the range $\beta = 0.2$–0.3, and $\alpha = 0.8$–0.9, we do not wish to de-emphasize the importance of deposition details. We therefore include a data set (Fig. 3, circles) recorded in identical conditions to that represented by the squares, except for the lack of a sample shutter to control the deposition rate during the initial stages of growth, and more frequent interruptions

of the deposition to prevent sample heating. Correlation lengths and saturated rms widths are significantly lower for the latter data set. We emphasize that details of the deposition process can have a great impact on the extent to which spatial correlations can develop, if not the mode of film growth itself.

Let us now compare our experimental results with current theories of nonequilibrium film growth. Such a comparison involves theories which treat homoepitaxial film growth on an initially flat surface while our experiment involved heteroexpitaxial growth. This issue has recently been examined in great detail within the context of CuCl growth on $CaF_2(111)$ [24], where it was concluded that kinetic growth theories could indeed be applied to heteroepitaxial growth conditions. In the following paragraph, we examine the consistency of the experimental roughness amplitudes with theory [25]. This is due to the fact that experiments have been known to compare favorably with theory in terms of the scaling exponents, yet exhibit roughness amplitudes which were seemingly inconsistent with theory [9,26].

The distance d that a particle travels before being incorporated into the surface can be very roughly estimated by assuming that $\sigma(d) \equiv 0.5a$ and writing the spatial scaling relation as $\sigma(L) = A(L/d)^{\alpha}$, with $a \approx 0.23$ nm being the size of one atomic step. In combination with the experimental observation that $\sigma(L) = 0.06L^{0.82}$, this assumption yields $d \approx 2$ nm. The width expected to develop over a 2 nm by 2 nm area on account of fluctuations alone [27], $\sqrt{h/a}/(d/a)$, is observed to be larger than $\sigma(d) \equiv 0.5a = 0.115$ nm for all values of h which were studied, consistent with the basic theoretical scenario whereby surface morphology results from a competition between random fluctuations in the incoming flux, $\eta(x, y, t)$ and surface smoothing processes such as diffusion effects.

The exponents which we observe are relatively close to predictions of the "pure diffusion" equation, $\partial h/\partial t = R_d + \eta - \kappa_1(\nabla^4 h)$, where R_d is the deposition rate and κ_1 is a smoothing prefactor: $(\alpha, \beta, z) = (1, 1/4, 4)$ [27], but these exponents are only expected in the preasymptotic scaling regime. They are also relatively close to the predictions of an equation presented recently by Siegert and Plischke [28], where additional terms in ∇h were included to refine the description of the surface morphology: $(\alpha, \beta, z) = (1, \frac{1}{4} - \frac{1}{3}, 3 - 4)$, for systems with positive Schwoebel barriers. Pyramidlike growth, which would be expected for the "growth instabilities" associated with $\alpha = 1$ is not, however, in evidence in the STM images. The observed roughness exponents moreover are not within experimental error of $\alpha = 1$, and the correlation lengths are observed to be of the same order as the crystalline grain sizes, which have been completely neglected by theory. Although there is growing experimental consensus that a wide range of deposition conditions can result in film growth characterized by $\beta = 0.2$–0.3; $\alpha = 0.8$–0.9, a gap remains between theory and experiment.

We gratefully acknowledge support from NSF Grant No. DMR-92-04092 and PRF Grant No. 27498-AC5.

[1] B. B. Mandelbrot, *The Fractal Geometry of Nature* (Freeman, New York, 1982).
[2] F. Family and T. Vicsek, *Dynamics of Fractal Surfaces* (World Scientific, Singapore, 1991).
[3] F. Family and T. Vicsek, J. Phys. A **18**, L75 (1985).
[4] J. Krim and J. O. Indekeu, Phys. Rev. E **48**, 1576 (1993).
[5] M. Kardar, G. Parisi, and Y.-C. Zhang, Phys. Rev. Lett. **56**, 889 (1986).
[6] P. Meakin, P. Ramandal, L. M. Sander, and R. C. Ball, Phys. Rev. A **34**, 5091 (1986); J. M. Kim and J. M. Kosterlitz, Phys. Rev. Lett. **62**, 2289 (1989); B. M. Forrest and L.-H. Tang, Phys. Rev. Lett. **64**, 1405 (1990).
[7] For recent reviews, see J. Krug and H. Spohn, in *Solids Far from Equilibrium: Growth Morphology and Defects,* edited by C. Gordreche (Cambridge University Press, Cambridge, 1991); P. Meakin, Phys. Rep. **235**, 191 (1994).
[8] H. Yan, Phys. Rev. Lett. **68**, 3048 (1992); D. A. Kessler, H. Levine, and L. M. Sander, Phys. Rev. Lett. **69**, 100 (1992).
[9] *Surface Disordering: Growth, Roughening and Phase Transitions,* edited by R. Julien, J. Kertesz, P. Meakin, and D. E. Wolf (Nova Science, Commack, 1992).
[10] S. Das Sarma, C. J. Lanczycki, S. V. Ghaisas, and J. M. Kim, Phys. Rev. B **49**, 10 693 (1994).
[11] H. You, R. P. Chiarello, H. K. Kim, and K. G. Vandevoort, Phys. Rev. Lett. **70**, 2900 (1993).
[12] C. Thompson, G. Palasantzas, Y. P. Feng, S. K. Sinha, and J. Krim, Phys. Rev. B **49**, 4902 (1994).
[13] Y.-L. He, H.-N. Yang, and T.-M. Lu, Phys. Rev. Lett. **69**, 3770 (1992).
[14] H.-J. Ernst, F. Fabre, R. Folkerts, and J. Lapujoulade, Phys. Rev. Lett. **72**, 112 (1994).
[15] G. W. Collins *et al.,* Phys. Rev. Lett. **73**, 708 (1994).
[16] V. Panella and J. Krim, Phys. Rev. E **49**, 4179 (1994).
[17] G. Rosenfeld, R. Servaty, C. Teichart, B. Poelsema, and G. Comsa, Phys. Rev. Lett. **71**, 895 (1993).
[18] G. Palasantzas and J. Krim, Phys. Rev. B **48**, 2873 (1993).
[19] G. Palasantzas, Phys. Rev. B **48**, 14 472 (1993); Eq. 4.10. $\sigma_2(L, h)$ is obtained from the analytic form $\sigma(L) = \sigma L^{\alpha}[L^2 + 2\pi^2\xi^2/\alpha]^{-\alpha/2}$ after substitution of $\sigma \propto t^{\beta}$, and $\xi \propto t^{\beta/\alpha}$.
[20] C. Thompson (private communication).
[21] J. Krim, I. Heyvaert, C. Van Haesendonck, and Y. Bruynseraede, Phys. Rev. Lett. **70**, 57 (1993).
[22] J. Chevrier, V. L. Thanh, R. Buys, and J. Derrien, Europhys. Lett. **16**, 737 (1991).
[23] R. C. Salvarezza, P. Vasquez, P. Herrasti, P. Ocon, J. M. Vara, and A. J. Arvia, Europhys. Lett. **20**, 727 (1992).
[24] W. M. Tong, R. S. Williams, A. Yanase, Y. Segawa, and M. S. Anderson, Phys. Rev. Lett. **72**, 3374 (1994).
[25] The analysis follows an approach outlined by J. Villain (private communication).
[26] R. Chiarello, V. Panella, J. Krim, and C. Thompson, Phys. Rev. Lett. **67**, 3408 (1991).
[27] J. Villain, J. Phys. I (France) **1**, 19 (1991).
[28] M. Siegert and M. Plischke, Phys. Rev. Lett. **73**, 1517 (1994).

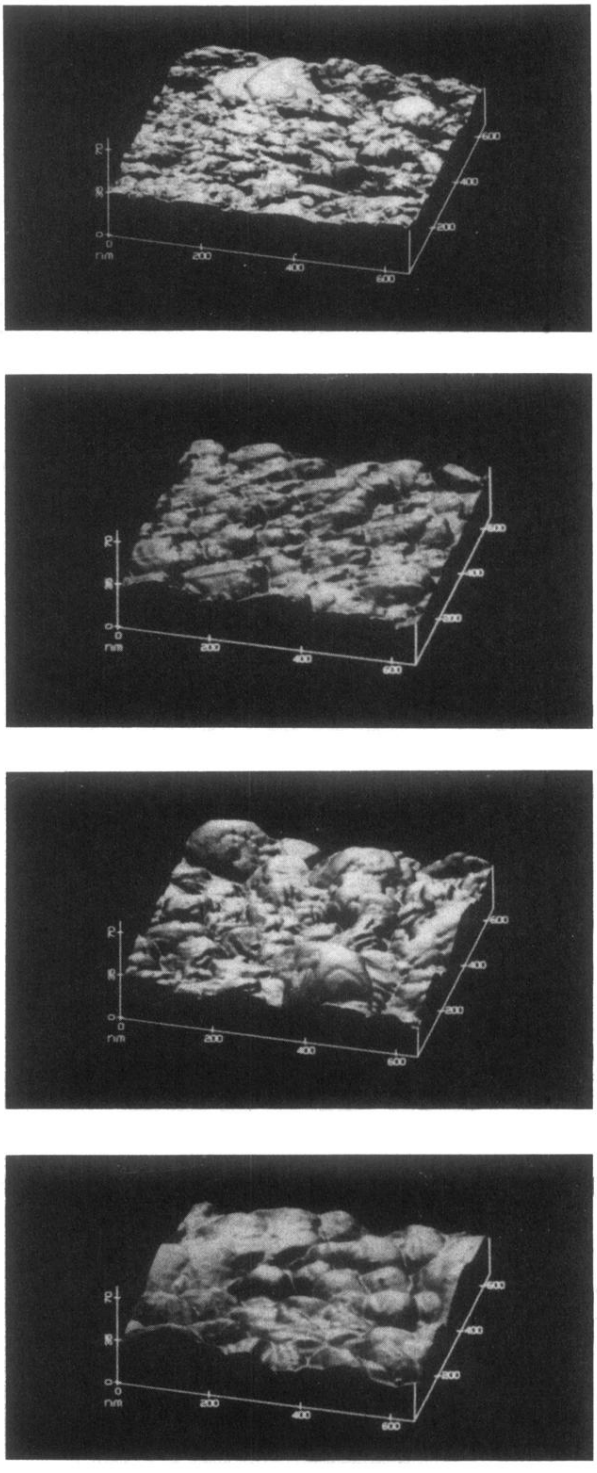

FIG. 1. Typical STM images for film thickness (top to bottom) $h = 50.2$, 147, 280, and 702 nm. The horizontal and vertical axes, respectively, range from 0 to 650 nm and 0 to 70 nm, so vertical fluctuations are magnified by approximately 3.